Development 138, 2883-2893 (2011) doi:10.1242/dev.055681

Serial specification of diverse neuroblast identities from a neurogenic placode by Notch and Egfr signaling

Helen J. Hwang[1,2] and Eric Rulifson[2,*]

SUMMARY

We used the brain insulin-producing cell (IPC) lineage and its identified neuroblast (IPC NB) as a model to understand a novel example of serial specification of NB identities in the *Drosophila* dorsomedial protocerebral neuroectoderm. The IPC NB was specified from a small, molecularly identified group of cells comprising an invaginated epithelial placode. By progressive delamination of cells, the placode generated a series of NB identities, including the single IPC NB, a number of other canonical Type I NBs, and a single Type II NB that generates large lineages by transient amplification of neural progenitor cells. Loss of Notch function caused all cells of the placode to form as supernumerary IPC NBs, indicating that the placode is initially a fate equivalence group for the IPC NB fate. Loss of Egfr function caused all placodal cells to apoptose, except for the IPC NB, indicating a requirement of Egfr signaling for specification of alternative NB identities. Indeed, both derepressed Egfr activity in *yan* mutants and ectopic EGF activity produced supernumerary Type II NBs from the placode. Loss of both Notch and Egfr function caused all placode cells to become IPC NBs and survive, indicating that commitment to NB fate nullified the requirement of Egfr activity for placode cell survival. We discuss the surprising parallels between the serial specification of neural fates from this neurogenic placode and the fly retina.

KEY WORDS: *Drosophila*, Egfr, Notch, Insulin, Neuroblast, Neurogenesis

INTRODUCTION

Regional molecular specification of the central nervous system (CNS) and anterior ectodermal placodes is evolutionarily conserved between flies and mammals (de Velasco et al., 2007; Wang et al., 2007; Lichtneckert and Reichert, 2008). The head neuroendocrine system largely arises from the anterior ectodermal placodes (Kawamura et al., 2002; Markakis, 2002; Whitlock, 2005), but details of specification mechanisms operating at a single-cell resolution are not known. In this study, *Drosophila* insulin-producing cells (IPCs), which express several *Drosophila* insulin-like peptides (Dilps), provide an excellent model to interrogate the specification of the brain neuroendocrine system from a placodal neuroepithelium.

Specification mechanisms that diversify the types of neurons and glia made during CNS development contribute to its extraordinarily complex architecture and functionality. In both vertebrates and invertebrates this process involves a neuroepithelium that specifies neural stem cells, or neuroblasts (NBs), which harbor distinct identities (Broadus et al., 1995; Qian et al., 1998). In one well-studied model of embryonic *Drosophila* neurogenesis, specification of NB identity within the ventral neuroectoderm (vNE) depends on the dorsoventral and anteroposterior axial patterning systems to generate a highly regionalized vNE that has been likened to a Cartesian coordinate map (for reviews, see Skeath, 1999; Skeath and Thor, 2003). At the onset of vNE neurogenesis, neighboring neuroepithelial cells that harbor a common regional identity, or map address, begin to express the proneural genes of the *achaete-scute complex* (*as-c*) (Martin-Bermudo et al., 1991; Skeath and Carroll, 1992) and thus comprise equivalence groups of 5-7 cells competent to form NBs. Once cells are competent, a lateral signal mediated by the Notch receptor and its ligand, Delta, acts through the *Enhancer of split* [*E*(*spl*)] family of proneural gene repressors to allow delamination of a single NB while specifying the remaining competent cells as epidermis (Lehmann et al., 1983; Technau and Campos-Ortega, 1987; Skeath and Carroll, 1992). The identified NBs acquire their distinct lineage properties from the factors that they inherit from the regionalized vNE (for reviews, see Bhat, 1999; Technau et al., 2006). This mode of NB specification extends to the ~100 identified procephalic NBs derived from the procephalic neuroectoderm (pNE), which form most of the brain (Urbach and Technau, 2003; Urbach et al., 2006; Urbach and Technau, 2008).

In contrast to the Cartesian map paradigm for NB identity specification within a sheet of NE, additional brain NBs, including those that generate the IPCs, derive from placodes in the head midline dorsomedial procephalic (Pdm) NE, where the neuroepithelium loses its sheet-like morphology preceding neurogenesis. The placodal Pdm NE forms invaginated vesicles of neurogenic cells characterized by a condensation of apical membranes and the expression of proneural factors. Unlike most of the NE, the invaginated Pdm neuroepithelium is neurogenic, such that adjacent competent cells all become NBs and not epidermis (Younossi-Hartenstein et al., 1996; de Velasco et al., 2007), a pattern that more closely parallels vertebrate CNS neurogenesis. Some regions of the pNE are neurogenic but do not form invagination centers (Urbach et al., 2003).

[1]Biomedical Sciences Graduate Program, UCSF, University of California San Francisco, San Francisco, CA 94143, USA. [2]Eli and Edythe Broad Center of Regeneration Medicine and Stem Cell Research at UCSF, University of California San Francisco, San Francisco, CA 94143, USA.

*Author for correspondence (eric.rulifson@ucsf.edu)

Accepted 22 April 2011

The Pdm contains diverse NB lineage identities, including Type I NBs, which divide in an asymmetric stem-cell mode to generate neural precursors called ganglion mother cells (GMCs), which in turn divide symmetrically to generate neurons (Boone and Doe, 2008). Pdm Type I NB identities include NBs for brain neurosecretory cell (NSC) lineages such as IPCs (Wang et al., 2007) and NBs for cholinergic neuron lineages (de Velasco et al., 2007; Wang et al., 2007). The Pdm also contains Type II NBs, also known as posterior Asense-negative (PAN) NBs, which produce transient-amplifying GMCs. These NB lineages can exceed 400 cells and comprise both neurons and glia (Pereanu and Hartenstein, 2006; Sprecher et al., 2007; Bello et al., 2008; Boone and Doe, 2008; Bowman et al., 2008; Izergina et al., 2009). Although several genes (*tailless*, *giant*, *lethal of scute*) are known to be crucial for specification of the pars intercerebralis (PI) (Younossi-Hartenstein et al., 1996; Younossi-Hartenstein et al., 1997; de Velasco et al., 2006) and Epidermal growth factor receptor (Egfr) activity is essential for Pdm cell survival (de Velasco et al., 2007), it is not known how these diverse NB identities are specified within neurogenic Pdm placodes.

In this study we investigate the role of Notch and Egfr signaling in the specification of the IPC NB and other NB identities from a molecularly identified 8-cell Pdm placode corresponding to the medial PI primordium (pPIm). The embryo produces only one IPC NB per brain hemisphere (Wang et al., 2007). We find that the 8-cell pPIm produces diverse NB identities including the IPC NB, several Type I NBs for small cholinergic neurons and a single Type II/PAN NB, which are formed in that sequence. In the absence of Notch signaling all pPIm cells delaminate as IPC NBs, indicating that the pPIm begins neurogenesis as a fate equivalence group for IPC NB identity. In the absence of Egfr signaling all cells of the pPIm, except the IPC NB, are lost by apoptosis, indicating that Egfr activity maintains cell survival in the remaining placode cells, which allows for the specification of later-specified NB identities. By contrast, the absence of both Notch and Egfr activity allows all pPIm cells to survive but they acquire the IPC NB fate, suggesting that the IPC NB identity, or NB fate in general, releases cells from the requirement of Egfr activity for survival.

MATERIALS AND METHODS

Fly stocks

All stocks were obtained from Bloomington Stock Center unless otherwise noted. Homozygous mutant embryos were identified using GFP-expressing balancer chromosomes. *Drosophila* strains included *yw* (used as the normal control genotype), N^{ts1}, N^{55e11}, Dl^{6B}, Dl^{RF}, $Egfr^{f24}$, $Egfr^{ts1a}$, *spi*^{1}, $Chx1^{A23}$ (*dchx1*^{A23}, gift of T. Erclik and H. Lipshitz, University of Toronto), *hh*^{21}, *dpp*^{h46}, *cas*^{24}, *chn*^{ECJ1} [gift of J. Modollel and S. Campuzano (Culi et al., 2001)], *phyl*^{2245}, *ttk*^{1e11}, *E(spl)m8-GFP* [gift of J. Posakony (Castro et al., 2005)], *dimm(c929)-GAL4, UAS-mCD8-GFP* [gift of R. Hewes (Hewes et al., 2003)], *rho-lacZ* (*rho*^{6}) (Bier et al., 1990), *rho*^{7m43}, *rho*^{7m}*vn*^{Ry} (Spencer et al., 1998), *UAS-rho* (gift of E. Bier, University of California, San Diego), *aop*^{1}, *pnt*^{d88}, *UASΔEN* (Larkin et al., 1996), *tll*- and *gt-GAL4* transgenes (gift of S. Celniker, Lawrence Berkeley National Laboratory), *mzVUM-GAL4, UAS-mGFP* (de Velasco et al., 2007) and *w; Act5C<stop>lacZ; UAS-flp* (Struhl and Basler, 1993).

Immunohistochemistry

Primary antibodies used were: mouse anti-Fas2 diluted 1:10 [mAB1D4; Developmental Studies Hybridoma Bank (DSHB)]; guinea pig anti-Chx1 1:500 (gift of H. Lipshitz); rabbit anti-Optix 1:500 (gift of F. Pignoni, Harvard University, Boston); mouse anti-Eya 1:250 (mAB10H6; DSHB); rat anti-Six4 1:25 (see below); chick anti-GFP 1:250 (Abcam); mouse anti-Crb (mABCq4; DSHB); rat anti-Dpn 1:1 (gift of C. Doe, University of Oregon, Eugene); mouse anti-Dac 1:100 (mABdac2-3; DSHB); rabbit anti-Cas 1:5000 (gift of W. Odenwald, National Institute of Health, Bethesda); guinea pig anti-Dimm 1:200 (gift of P. Taghert, Washington University, St Louis); rabbit anti-CC3 1:50 (Cell Signaling Technology); mouse anti-pMAPK 1:10 (Sigma); guinea pig anti-Ase 1:100 (gift of Y. N. Jan, University of California, San Francisco); and rabbit anti-Mir 1:1000 (gift of Y. N. Jan). Secondary antibodies (Jackson ImmunoResearch) were conjugated to Dylight 488, 549, 594 and 750 (Pierce) and Alexa Fluor 647 fluorescent conjugates (Invitrogen) diluted 1:1000. Multiplex images were obtained using a Zeiss Axioimager Z1 equipped with Exfo X-CITE illumination, a Photometrics HQ2 CCD camera and Semrock FISH dichroic filter sets; images were acquired in Axiovision 4.8 (Zeiss) and figures were produced with Photoshop CS4 (Adobe).

Temperature shift regimes

For temperature shift experiments, $Egfr^{ts}$ ($Egfr^{ts1a}/Egfr^{f24}$), $Delta^{ts}$ (Dl^{6B}/Dl^{RF}) and $Notch^{ts}$ (N^{ts1}/N^{55e11}) embryos were reared at the permissive temperature (18°C) and then subject to a 3- or 6-hour shift at the restrictive temperature (29°C). Embryos were either fixed immediately following the temperature shift, or were further incubated for 6 hours at the permissive temperature. For analysis of Optix and Dimm expression, $Delta^{ts}$ embryos were reared entirely at the restrictive temperature and examined at stage 17. Brains were dissected from first instar $Delta^{ts}$ mutants subjected to a 4-hour temperature shift as embryos and then reared at the permissive temperature to stage L1.

BrdU labeling

For pulse labeling with 5-bromodeoxyuridine (BrdU), embryos were permeabilized with octane then incubated for 2 hours in 1×PBS containing 1 mg/ml BrdU (Sullivan et al., 2000). Embryos were then fixed and blocked as described above. Prior to immunostaining, embryos were treated with 50 units/ml DNaseI (Roche) for 90 minutes in a 37°C water bath.

Antibody production and purification

A fragment from the predicted *Six4* ORF was amplified by PCR using primers 5′-GGGGAATTCCATCAGGACAATCTCAGCTCG-3′ and 5′-GGGCTCGAGGGTGATGTCCTGAAACCGCC-3′ and was cloned into pGEX (Novagen) to produce a GST fusion protein with the following peptide: HQDNLSSPMAYGSLFLPNAGYRGNLSCKTVLQLDKFAPY-EGVEKDHLLERRFQDIT. The fusion protein was purified using the B-PER GST Fusion Protein Purification Kit (Thermo Scientific) and used to immunize rats. Antibody production was performed by Josman (Napa, CA, USA). Bleeds were purified using the Melon Gel IgG Spin Purification Kit (Thermo Scientific).

RESULTS

The Pdm placode system expresses placode genes

The Pdm NE comprises three molecularly identified subdivisions: the pars intercerebralis primordium (pPI), which is demarcated by expression of the transcription factor Chx1; the pars lateralis primordium (pPL), which is demarcated by expression of the cell adhesion molecule Fas2; and the pars medialis primordium (pPM) domain, which is defined by expression of the transcription factor Rx (de Velasco et al., 2007) (Fig. 1A). The PI and PL contain the NSCs that form the brain-ring gland complex (Siegmund and Korge, 2001; de Velasco et al., 2007; Park et al., 2008). At stage 11, the greater Pdm placode system, which comprises the pPI, pPL and pPM, was demarcated by dorsoanterior head expression of the transcription factors Six4 and Eya. Oddly, Eya expression was evident in all pPI cells at stage 10, but was then diminished in the pPIm by stage 11 (see Fig. S1A in the supplementary material). The $Chx1^{+}$ pPI and $Fas2^{+}$ pPL were demarcated by Optix expression (see Fig. S1B in the supplementary material, which shows a stage 11 lateral view, Fig. S1C a stage 14 dorsal view), where it overlapped with Six4 expression (see Fig. S1A in the supplementary material).

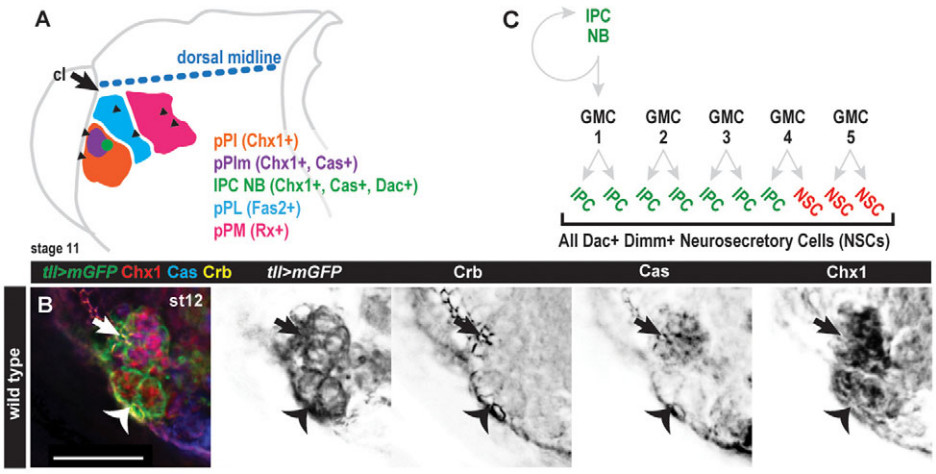

Fig. 1. The IPC NB is produced by a molecularly distinct pPIm placode. (**A**) A color-coded regional map of the *Drosophila* Pdm neuroectoderm (NE) in dorsolateral view (dorsolateral orientation is the same in subsequent figures). The Pdm NE includes the embryonic primordia of the pPI, pPL and pPM. Arrowheads mark the position of individual apical constrictions. The pPIm (purple) specifically expresses Chx1 and Cas. The insulin-producing cell neuroblast (IPC NB, green) is uniquely identified by the co-expression of Dac. (**B**) *tll>mGFP* outlines cellular boundaries in the Pdm NE. Accumulated Crb expression marks apical constrictions. Arrow, pPIm; arrowhead, adjacent Cas$^-$ pPI placode. (**C**) The IPC NB lineage of neurosecretory cells. cl, clypeolabral furrow; GMC, ganglion mother cell; pPI, pars intercerebralis primordium; pPIm, medial pars intercerebralis primordium; pPL, pars lateralis primordium; pPM, pars medialis primordium. Scale bar: 20 μm.

At stage 11, the cellular localization of a transgene reporter for Notch activity in the Pdm, *E(spl)m8-GFP* (*m8-GFP*) (Castro et al., 2005), highlighted the boundaries of discrete epithelial vesicles just beneath the outer epithelium, which revealed the structure of placodal cell groups that frequently had a visible apical epithelial constriction (see Fig. S1D in the supplementary material). These results show that the domain of overlapping expression of the evolutionarily conserved anterior 'placode genes' (Schlosser, 2006) *Six4*, *Optix* and *eya* demarcated a system of individual placodes (see Fig. S1D in the supplementary material). Within the system of placodes, the pPIm, a cluster of NE cells that are specifically Castor (Cas)$^+$ (Cui and Doe, 1992) and Chx1$^+$, formed a morphologically distinct and coherent structure bearing a single apical constriction (Fig. 1B).

In addition to defining structural features, we also found that cells recruited to the pPIm underwent a round of synchronous cell division prior to invaginating, implying their early developmental coordination (see Fig. S2A-C in the supplementary material). Moreover, the timing of Notch and Egfr pathway activation was coordinated as well (see Fig. S2D-F in the supplementary material). These results indicated that the pPIm showed placode-autonomous development relative to neighboring Pdm placodes.

Neurogenesis of identified NBs from the pPIm placode

At stage 11 of embryogenesis (Campos-Ortega and Hartenstein, 1985) placode formation is accompanied by the onset of pan-placodal expression of the proneural factor Lethal of scute, which is essential for neurogenesis (Younossi-Hartenstein et al., 1996). Additionally, several Notch signaling target genes of the *E*(*spl*)-*C* family, including *m5* and *m8*, are activated at this time (Tomancak et al., 2002; de Velasco et al., 2007). Notch activity persists for several hours, roughly spanning stages 11 through 14, while NBs continue to delaminate in an orderly succession. This process proceeds until the placodal NE cells at the epithelial surface are depleted by NB formation as cells release the constricted apical adherens junction and delaminate basally into the interior (Younossi-Hartenstein et al., 1996; de Velasco et al., 2007).

The IPCs are the only NSCs or neurons of the PI or PL for which lineage-tracing analysis has identified a progenitor, the IPC NB, which is a unique Dachshund (Dac)$^+$, Cas$^+$ and Chx1$^+$ cell in its region (Wang et al., 2007). The IPC NB is a canonical Type I NB (Boone and Doe, 2008), which divides asymmetrically to produce 5-6 GMCs that divide again symmetrically to generate a lineage of 10-12 NSCs by the end of embryogenesis; 6-8 of these NSCs are IPCs whereas the remainder remain unidentified by neuropeptide (Wang et al., 2007) (Fig. 1C).

Within the pPIm only the IPC NB lineage produces NSCs. We followed expression of Dimmed (Dimm), a determinant of NSC differentiation (Park et al., 2008), in the IPC NB lineage of stage 17 embryos, which is before the cells express Dilps (Rulifson et al., 2002), using a *dimm*-GAL4 transgene that drives membrane-bound GFP in NSCs (*dimm*-GFP) (Park et al., 2008). We found that the entire pPI, as labeled by Chx1 expression, contained two groups of Dac$^+$ and *dimm*-GFP-expressing cells, the larger and posterior of which were of the IPC NB lineage, as previously shown by clonal analysis (Wang et al., 2007) (see Fig. S3A in the supplementary material). We also labeled the IPC NB lineage by Dac and Dilp2 (Ilp2 – FlyBase) expression in the first instar larval brain and found that, at this stage, the IPC NB lineage remained the only NSC group in the close vicinity (see Fig. S3B in the supplementary material).

We investigated the birth order of the IPC NB from the pPIm by quadruple labeling embryos for expression of Dac, Cas, Chx1 and the NB marker Deadpan (Dpn) (Bier et al., 1992). Before delamination of NBs from the pPIm began (stage 11), Dpn was transiently elevated in the pPIm NE cells, which were still tethered to the outer epithelium at their apical constriction (Fig. 2A; asterisk marks the apical constriction). Once NBs began to delaminate, placodal Dpn expression was lost and Dpn was elevated in newly forming NBs, which resided basal to the placodal NE cells.

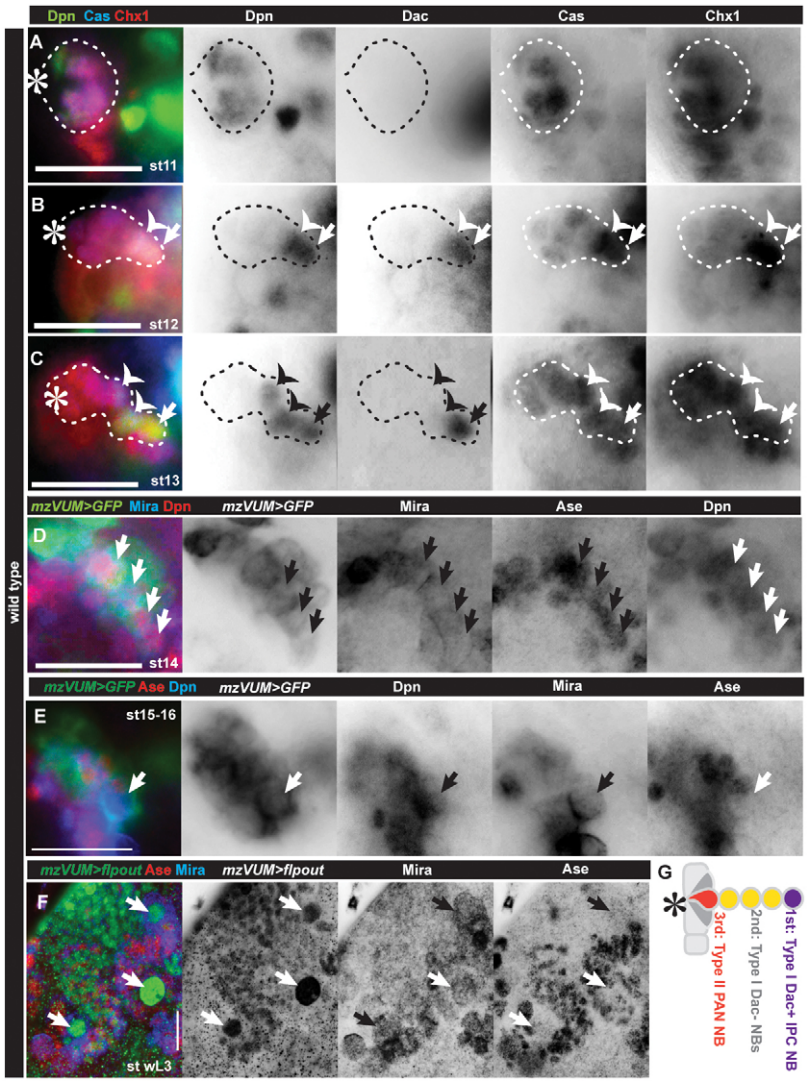

Fig. 2. Neurogenesis of diverse NB identities from the pPIm. (**A-C**) Dorsolateral view of embryo (anterior left) showing the pPIm (Cas$^+$ Chx1$^+$, outlined) and the site of apical constriction (asterisk). (A) Prior to the onset of neurogenesis, placodal neuroepithelial cells express transient low levels of Dpn. (B,C) High levels of Dpn mark newly formed NBs. The first-born IPC NB is the posterior-most of two pPIm NBs at stage 12 (B, arrow; non-IPC NB, arrowhead) and of three NBs at stage 13 (C, arrow; non-IPC NB, arrowheads). (**D-F**) *mzVUM-GFP* expression marks the pPI. (D) Four Type I NBs (Mira$^+$ Dpn$^+$ Ase$^+$) are present in the pPIm at stage 14 (arrows). (E) A single Type II NB (Mira$^+$ Dpn$^+$ Ase$^-$) is found in the pPIm in stage 15-16 *Drosophila* embryos. (F) Marked lineages of the pPI NE include three Type II NBs (arrows) and their respective lineages in a wandering third instar (wL3) brain. (**G**) Summary of pPIm NB birth order. Scale bars: 20 μm.

Although the IPC NB formed at the onset of stage 12, it became Dac$^+$ ~2 hours later, at late stage 12 (Fig. 2B,C, arrow). The IPC NB was stereotypically positioned at the posterior tip of a row of two or three pPIm NBs that had formed (Fig. 2B,C, arrowheads), suggesting that it was the first to be specified as an NB.

To confirm that the diverse NB identities in the Pdm are the products of a single placode we examined the non-IPC NBs within the pPIm for Type I and Type II NB expression profiles. Type I NBs express Dpn, Miranda (Mira) and Asense (Ase), whereas Type II NBs (PAN NBs) express Dpn and Mira but not Ase (Boone and Doe, 2008; Bowman et al., 2008). The *mzVUM-GAL4* and *UAS-mCD8 GFP* (*mzVUM-GFP*) transgene combination labels the pPI (de Velasco et al., 2007) and we identified the pPIm as the Cas$^+$ posterior region of the Chx1$^+$ *mzVUM-GFP* domain (see Fig. S3C in the supplementary material). Using *mzVUM-GFP* to mark the pPIm, we found that the NBs formed by the pPIm immediately following the IPC NB, at stage 14, are also Dpn$^+$ Mira$^+$ Ase$^+$ Type I NBs (Fig. 2D). However, by late stage 15, the pPIm contained a single Dpn$^+$ Mira$^+$ Ase$^-$ Type II NB (Fig. 2E). We never observed more than a single Type II NB within the pPIm and it appeared at the end of pPIm neurogenesis. To confirm that this NB generates a Type II lineage, which proliferates extensively in the third instar (Boone and Doe, 2008), we combined *mzVUM-GAL4* and *Act5C<stop>lacZ; UAS-flp* (Struhl and Basler, 1993) to permanently mark the lineages of the pPI in third instar larval brains. We found that at least two Type II NB lineages are marked (Fig. 2F). The example shows three widely spaced Type II NBs; most commonly, there were only two Chx1$^+$ Type II NBs per hemisphere (11/12 cases examined). The presence of marked lineages in the larval PI suggests that the identified Ase$^-$ pPIm NB does indeed give rise to a Type II NB lineage. The model of pPIm NB birth order is summarized in Fig. 2G.

The pPIm placode is an equivalence group for the IPC NB fate

Our observations that the IPC NB is the first fate specified from the pPIm and that activation of Notch pathway targets temporally coincide with IPC NB specification led us to examine the role of the Notch pathway in fate specification. We observed that a well-characterized zygotic *Notch* hemizygous male embryo (N^{55e11}/Y) (Rulifson and Blair, 1995), which receives two doses of maternal *Notch* mRNA from the compound balancer chromosome, gave the most severe loss-of-function phenotype where the pPIm could still be recognized. At late stage 12, the time of normal Dac$^+$ IPC NB appearance, most, if not all, Cas$^+$ Chx1$^+$ pPIm cells expressed high levels of Dpn and Dac, suggesting that they had mass delaminated

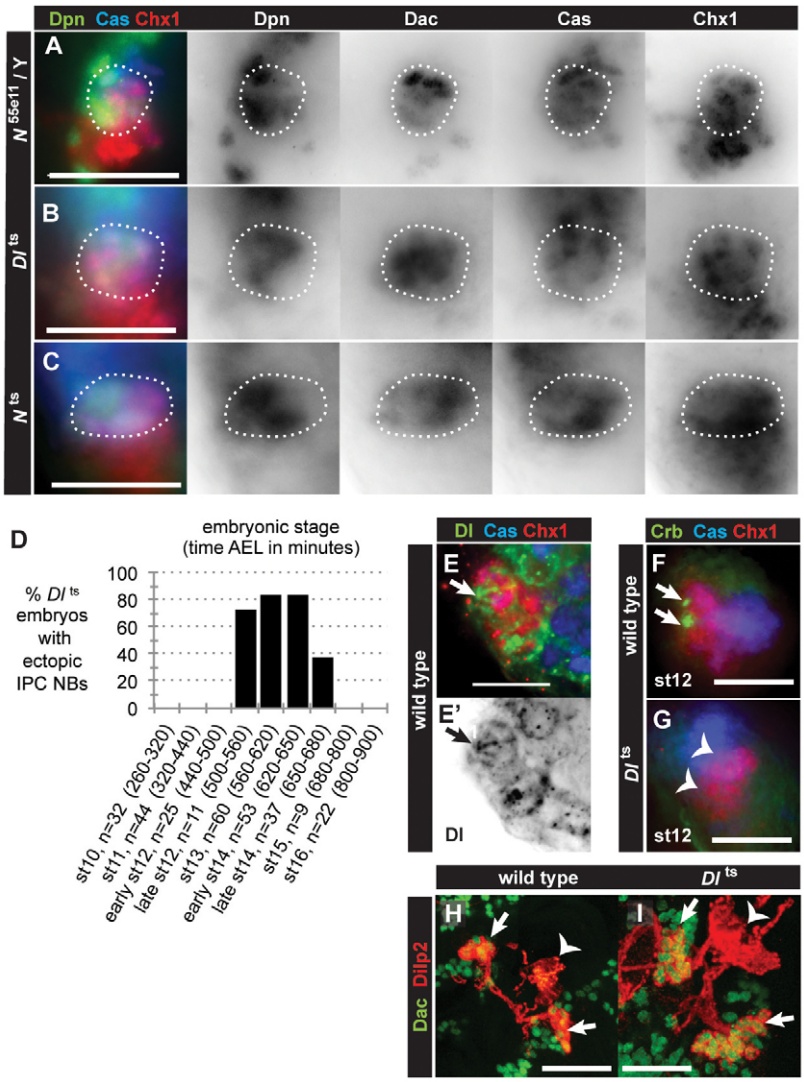

Fig. 3. The role of Notch signaling in IPC NB specification. (**A-C**) Supernumerary IPC NBs within the pPIm (outlined) at stage 13. (A) N^{55e11}/Y hemizygote; (B) *Delta*^{ts} after a 3-hour temperature shift; (C) *Notch*^{ts} after a 3-hour temperature shift. (**D**) Stage-by-stage quantification of ectopic IPC lineages in *Delta*^{ts} embryos subjected to a 3-hour temperature shift. (**E**,**E'**) In wild-type *Drosophila* embryos, Delta accumulates at the apical constriction of the pPIm (arrow). (**F**,**G**) Labeling of pPI apical constrictions by Crb at stage 12 in *Delta*^{ts}/+ heterozygous control ('wild type', F, arrows) and in *Delta*^{ts} after a 3-hour temperature shift (G, arrowheads). (**H**,**I**) IPCs in *Delta*^{ts}/+ heterozygous control and *Delta*^{ts} first instar larval brains following a 4-hour temperature shift during the competence period. Corpora cardiaca are marked by arrowheads. (H) Control brains with 6-8 Dac^{+} Dilp2^{+} IPCs per hemisphere. (I) *Delta*^{ts} brains with supernumerary Dac^{+} Dilp2^{+} IPCs. Scale bars: 20 μm.

as supernumerary IPC NBs (4/5 cases; Fig. 3A). The ectopic IPC NBs were judged to come from the pPIm because they occupied the same position as normal, they were the same in number as the Cas^{+} Chx1^{+} NBs found in the normal pPIm, and they remained as a contiguous group.

To further test the temporal requirements for Notch signaling we used temperature upshift experiments with temperature-sensitive (*ts*) genotypes of *Delta* (Dl^{RF}/Dl^{6B}=*Delta*^{ts}) (Parks et al., 2006) and *Notch* (N^{ts1}/N^{55e11}=*Notch*^{ts}) (Heitzler and Simpson, 1991). We examined the specification of IPC NB fate in *Delta*^{ts} embryos at stages 10 through 17 following a 3-hour shift from the permissive temperature of 18°C to the restrictive temperature of 29°C. Quadruple labeling for Dpn, Dac, Cas and Chx1 was used to follow cells with IPC NB identity. Following upshifts ending at stage 12-13, the time of normal IPC NB appearance, most, if not all, pPIm cells in upshifted *Delta*^{ts} (Fig. 3B,D) and *Notch*^{ts} (6/8 cases; Fig. 3C) embryos expressed high levels of Dpn and Dac, phenotypes that matched those of the *Notch* hemizygotes. *Notch*^{ts}/+ embryos provided controls for the effect of temperature shift and were normal (5/5 cases; see Fig. S4A in the supplementary material). When later stage *Delta*^{ts} embryos were scored for the presence of supernumerary IPC NBs and their lineages, we found that only stage 12 through stage 14 had supernumerary IPC NB lineages following the 3-hour shift, whereas stage 15 and later embryos were no different than controls. No ectopic Dac^{+} IPC NBs lineages were observed earlier than late stage 12 (Fig. 3D). A 3-hour upshift after 680 minutes of development produced no supernumerary IPC NBs; hence, the end of the competence period for pPIm cells to take the IPC NB fate occurs at 500 minutes of development, corresponding to the end of stage 12, when the IPC NB first expresses Dac. Consistent with a requirement for Delta, we observed that Delta protein accumulated on the placodal cells and was enriched at the apical constriction of the pPIm (Fig. 3E).

In both *Notch*^{ts} and *Delta*^{ts} embryos at early stage 12 or before, prior to the time of normal IPC NB appearance, there was no precocious differentiation of the Dac^{+} IPC NB. However, in stage 10-11 mutant embryos, most pPIm cells delaminated en masse and expressed a high level of Dpn, which indicated that in the absence of Notch activity near the time of onset for proneural gene expression all placodal NE cells became NBs (9/9 cases; see Fig. S4C in the supplementary material); no NBs formed in controls of a similar stage (see Fig. S4B in the supplementary material). Shifted *Delta*^{ts} embryos at the same stage also showed no apical Crb accumulation (Fig. 3G) when compared with controls (Fig. 3F), indicating that the delamination of placodal NBs was correlated with the loss of the apical adherens junction with the

outer epithelium. Thus, although the competence period to form an IPC NB ended near the time that the IPC NB normally first appears, Notch activity and neurogenesis in the pPIm placode persisted for at least 3 hours after this point, through the end of stage 14 (de Velasco et al., 2007).

In order to further test the fate equivalence of the induced supernumerary IPC NBs, we examined their potential to proliferate and differentiate as fully fledged IPCs. *Delta*^{ts} embryos were shifted for 3 hours to the restrictive temperature to induce supernumerary IPC NBs and then shifted back to permissive temperature and allowed to develop to stage 16. The Cas^{+} Chx1^{+} pPIm of stage 16 embryos were entirely composed of supernumerary Dac^{+} cells (3/3 cases; see Fig. S4E as compared with the control in S4D in the supplementary material). The volume of the Dac-expressing cell cluster, although difficult to quantify, was roughly six- to eightfold greater than in control embryos, as would be expected if the cluster arose from the proliferation of 6-8 IPC NB lineages. *Delta*^{ts} first instar larval brains harboring supernumerary IPC NB lineages induced by 4-hour temperature shifts delivered at stage 11-12 formed large clusters of supernumerary Dac^{+} and Dilp2^{+} NSCs that had larger than normal fascicles of cell processes that extended in the normal IPC projection pattern (Fig. 3I,H; 13/13 cases compared with 0/25 in normal control brains). Together, these results suggest that the pPIm placode is a group of roughly eight neuroepithelial cells, each possessing the equivalent developmental potential to become specified as an IPC NB at the appropriate time.

Given that the pPIm placode is only one of several that comprise the primordium of the PI and PL neuroendocrine center, we asked whether all pPI and pPL placodes are equivalence groups that produce a single NSC lineage NB and several non-neurosecretory lineage NBs. We first examined the expression of Dimm in the Optix^{+} pPI and pPL in late stage 17 *Delta*^{ts} embryos reared entirely at the restrictive temperature. In the absence of Notch activity, the pPI and pPL appeared expanded in size with a majority of ectopic Optix^{+} cells expressing Dimm (4/4 cases; see Fig. S4G as compared with the control in S4F in the supplementary material). We suspect that the increased size of the Optix^{+} domain was due to respecification of late-proliferating primary and secondary NBs to early-proliferating NSC NB primary lineages. Many of the ectopic Dimm^{+} cells within the pPI and pPL also expressed Dac, similar to the IPC NB lineages. The mass conversion of cell fates to NSCs was largely restricted to the pPI and pPL, with the exception of the neuroendocrine corpora cardiaca (CC) cells, which were also dramatically increased in number (see Fig. S4G, arrowhead, in the supplementary material). We previously proposed that the CC cells are produced from an NB lineage that arises adjacent to the pPIm in the same field of Eya and Six4 expression, although a placode for the CC NB has not been identified, in part because of the rapid migration of differentiating CC cells away from the placodal NE (Wang et al., 2007).

We analyzed the impact of increased transgenic Notch activity on IPC NB specification using a *giant* (*gt*) enhancer-GAL4 fusion transgene and the *UAS-Notch*^{act} intracellular fragment transgene (*UASΔEN*) (Larkin et al., 1996), which activates the Notch pathway in the Pdm NE. In contrast to Notch loss of function causing early NB formation, gain of Notch activity caused a delay in the specification of the IPC NB from late stage 12 (see Fig. S4H in the supplementary material; Dac^{+} IPC NB absent in 5/5 cases) to stage 14 (see Fig. S4I in the supplementary material; Dac^{+} IPC NB present in 9/21 cases). Although the IPC NB was ultimately specified, perhaps owing to a drop in transgene activity, this result suggests that the competence period for the IPC can be extended by at least 2 hours if Notch activity is maintained at a high level in the placode. This result is then also consistent with a role for IPC NB specification in closing the competence period in the pPIm.

Egfr signaling promotes the survival of non-neurosecretory pPIm lineages

Throughout Pdm neurogenesis, the EGF/TGFα homolog Spitz (Spi), Egfr activity and Ras activation maintain survival of placodal cells and ectopic Egfr/Ras pathway activation is sufficient to disrupt cell fate and proliferation within the placodal NE (Rogge et al., 1995; Dumstrei et al., 1998). Loss of Egfr activity results in an increase in apoptosis throughout the anterior placode system beginning at stage 12, with the pPI and pPL being severely reduced in size as shown by loss of Chx1^{+} and Fas2^{+} cells (Dumstrei et al., 1998; de Velasco et al., 2007; Park et al., 2008).

We examined whether, in addition to promoting cell survival, Egfr activity is essential for specification of the IPC NB or other NB identities in the pPIm. We first examined homozygous embryos of the well-characterized *Egfr*^{f24} null allele (Clifford and Schupbach, 1989). Surprisingly, we found that at stage 14 a single IPC NB was specified as normal, although there was reduction of the pPI to only a few cells overall (14/14 cases; Fig. 4A), which we suspect were the first NBs formed from adjacent pPI placodes. We compared the *Egfr*^{f24} mutant phenotype with another allelic combination, *Egfr*^{ts1a}/*Egfr*^{f24} (*Egfr*^{ts}), which is a functional null at 29°C (Kumar et al., 1998). In upshift studies that paralleled those performed with *Notch* and *Delta* alleles, we examined *Egfr*^{ts} embryos immediately following a 6-hour shift from 18°C to 29°C. We found that upshifted stage 12-13 embryos had the same phenotype as *Egfr*^{f24} mutants (6/9 cases compared with 0/5 cases for the control; Fig. 4B). However, embryos shifted at later stages exhibited a progressively reduced loss of pPI cells the later the shift occurred; at stage 17, there was no noticeable defect in the size of the pPI (0/5 cases, as with the control; Fig. 4C). These temperature shift results indicated that the commitment of pPIm cells to the NB fate abrogates the requirement for Egfr for survival. Consistent with this view, levels of pMAPK (Rolled – FlyBase), which is associated with activation of Egfr activity, were higher in pPIm placodal NE cells than in NBs (Fig. 4D).

Parallel results were seen with *spi*^{1} homozygous mutant embryos, where the IPC NB was specified but the remaining pPIm NE cells were absent (Fig. 4E). We examined whether the loss of pPIm cells and NBs was due to apoptosis, based on previous observations (Dumstrei et al., 1998; de Velasco et al., 2007). In early stage 11 *spi*^{1} embryos, the Chx1^{+} pPI was normal in size and showed no evidence of cell death (see Fig. S5B and compare with control in S5A in the supplementary material). However, in late stage 11 *spi*^{1} embryos we observed many Chx1^{+} cells with elevated cleaved Caspase 3 (CC3; Decay – FlyBase) and an overall reduction in the size of the pPI (Fig. 4G, compare with control in 4F). Control embryos also contained apoptotic cells but they were not Chx1^{+}; they were likely to be scavenging hemocytes that had phagocytosed apoptotic cells (arrows).

We further examined stage 14 *spi*^{1} embryos and stage 14 mutants of other Egfr pathway components. The pPI size was quantitated as the mean number of Dac^{-} Chx1^{+} cells per hemisphere (mean ± s.e.m.). The pPI was reduced from normal size (14.6±0.75 cells, *n*=5; see Fig. S5A in the supplementary material) in the following mutants: *spi*^{1}, 1.87±0.35, *n*=15 (Fig. 4E); *Egfr*^{f24}, 2.38±0.59, *n*=16 (Fig. 4A); *rho*^{7m43} [*rhomboid*, which encodes the

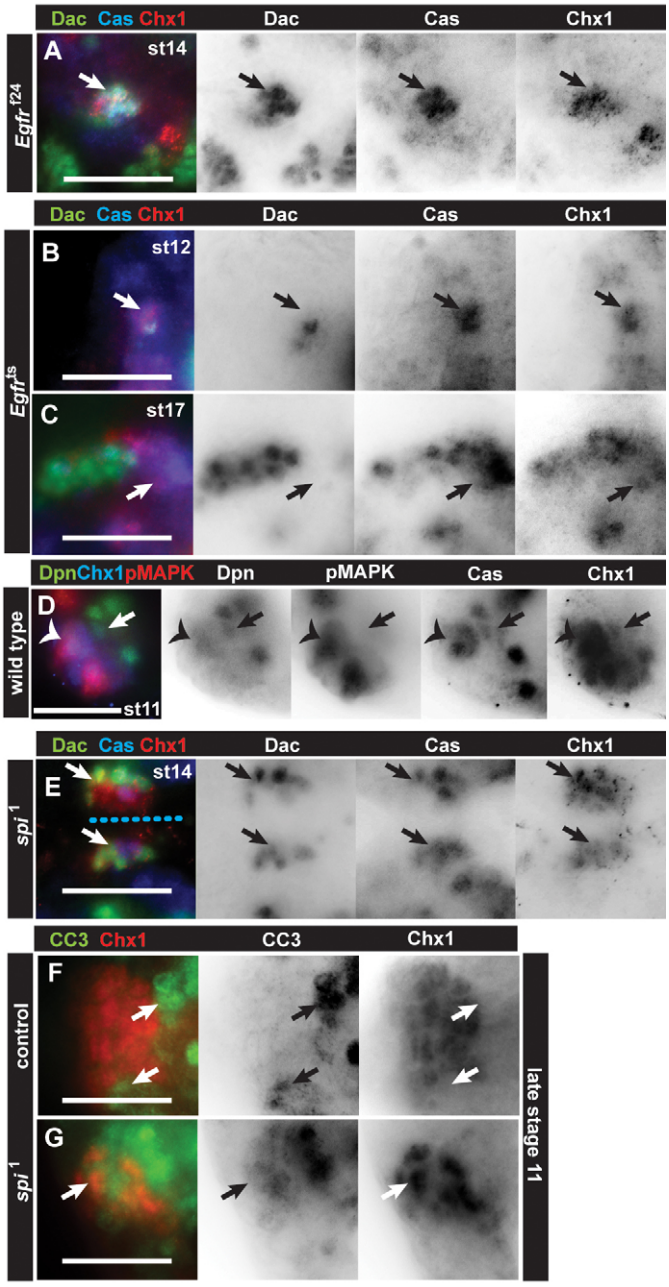

Fig. 4. Egfr activity is essential in pPIm NE for non-IPC NB survival. (**A**) The pPIm (arrows) in an *Egfr*^{f24} *Drosophila* embryo at stage 14 is reduced in size, but the Dac^{+} IPC lineage is present. (**B**,**C**) *Egfr*^{ts} after a 6-hour temperature upshift. (B) Stage 12 embryos with a reduced pPIm and (C) stage 17 embryos with a normal sized pPIm. (**D**) pMAPK, an indicator of activation of Egfr activity, is elevated in placodal pPIm NE cells (arrowhead), but is absent from NBs (arrow). (**E**) *spi*^{1} mutants show a comparable phenotype to the *Egfr*^{f24} mutants. The dashed blue line indicates the head midline. (**F**,**G**) Cell death in heterozygous control and *spi*^{1} embryos labeled by anti-CC3. The pPIm does not express CC3 in controls (F, arrows mark Chx1^{-} hemocytes adjacent to the pPI), but is labeled by anti-CC3 in *spi*^{1} embryos (G, arrow). Scale bars: 20 μm.

protease essential for activation of Spi signaling activity (Urban et al., 2002)], 2.93±0.29, *n*=15 (see Fig. S5C in the supplementary material); *rho*^{7m} *vn*^{ry} [a combined loss of Rho and Vein, a Rho-independent Egfr ligand of the neuregulin type (Schnepp et al., 1996)], 2.14±0.51, *n*=7 (see Fig. S5D in the supplementary material). This suggested that Spi was the ligand principally responsible for promoting Egfr-dependent non-IPC NB pPIm cell survival. Given that the IPC NB was specified normally in Egfr pathway mutants, we investigated whether Egfr activity is essential for the morphogenesis of placode formation. *spi*^{1} embryos made a pPIm apical constriction during stage 11 as normal (see Fig. S5E in the supplementary material), and similar results were observed with *Egfr*^{f24} homozygous embryos (not shown).

Egfr-dependent pMAPK activity leads to activation of the ETS domain transcriptional activators Pointed 1 (Pnt1) and Pnt2 (Scholz et al., 1993). We examined homozygous embryos with both the *pnt1* and *pnt2* genes deleted (*pnt*^{d88}) (Klaes et al., 1994) and found that by stage 14 there was no significant loss of cells from the pPIm and that the IPC NB lineage was specified normally (14/14 cases; see Fig. S5F in the supplementary material), which indicated that the cell survival signal was not principally transduced by *pnt1/2*. Thus, the suppression of cell death might come from an upstream pathway component such as MAPK or be exerted by an unidentified parallel pathway. Pnt activity is repressed by the ETS factor Yan (Aop), which is removed from the target gene enhancer and exported out of the nucleus following phosphorylation by pMAPK, which then allows Pnt1/2 to activate transcription (for a review, see Doroquez and Rebay, 2006). We examined the phenotype of *yan* homozygous mutants (*aop*^{1}). Loss of yan function leads to hyperplasia of the Pdm (Rogge et al., 1995), yet we found that the IPC NB was specified normally (5/5 cases; see Fig. S5G in the supplementary material). Interestingly, we found that in stage 15-17 embryos, loss of Yan led to specification of supernumerary Dpn^{+} Ase^{-} Type II NBs in the pPI (5/6 cases; see Fig. S5H in the supplementary material). Ectopic Spi activity induced using *gt-GAL4* and *UAS-rho* transgenes also produced supernumerary Type II NBs in the Optix^{+} Pdm (not shown). These results suggested that Spi/Egfr signaling might promote the Type II fate at the expense of non-IPC Type I NBs within the pPIm. Alternatively, remaining pPIm cells that would otherwise apoptose were directed to the Type II NB fate. Either way, the requirement for Yan and the effect of ectopic Spi implicate Egfr activity in pPIm cell fate specification beyond mere regulation of cell survival, which did not require Pnt1/2 function.

Crossregulation of Notch and Egfr pathways in the pPIm

Our observation that the IPC NB is the only pPIm cell to survive led us to question whether the commitment to the IPC NB, or simply an NB fate alone, is sufficient to prevent pPIm cells from ever becoming dependent upon Egfr activity for survival. We analyzed double-homozygous mutants for Spi and Delta (*spi*^{1}; *Dl*^{RF}), a strong hypomorphic allele combination at 29°C. Simultaneous loss of both Egfr and Notch activity led to a Notch phenotype, with supernumerary IPC NBs produced at the expense of other pPIm cells (15/20 cases; Fig. 5A). When Egfr pathway activity alone was lost we never observed a neurogenic effect in which NBs formed abnormally. Hence, Notch signaling does not critically depend on Egfr activity to be activated or maintained. We then tested whether Notch activity was required to activate Spi/Egfr signaling. We found that *Notch* hemizygous embryos were still able to activate Rho, as assayed by the *rho* transcriptional reporter *rho-lacZ* (Bier et al., 1990) (Fig. 5B). Additionally, in *Notch* hemizygotes, we also detected pMAPK in the pPIm (Fig. 5C). Conversely, the *m8-GFP* reporter of Notch activity was expressed in the pPI of *Egfr*^{f24} embryos (Fig. 5D).

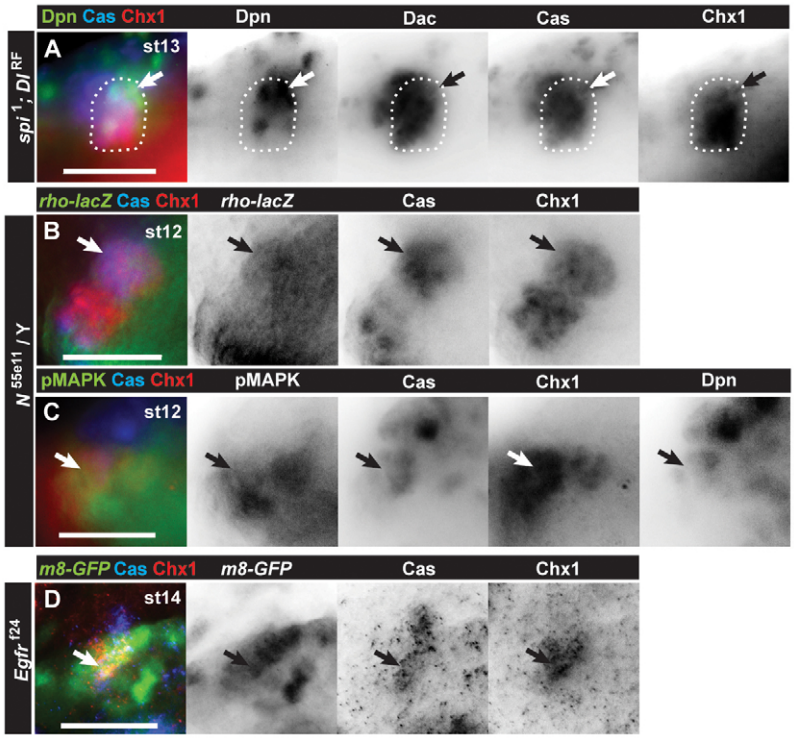

Fig. 5. Notch and Egfr in the pPIm are not mutually dependent. (**A**) Stage 13 *spi*^{1}; *Dl*^{RF} double mutants with a normal sized pPIm (outlined) and supernumerary IPC NBs (arrow). (**B**,**C**) Egfr activity in the pPIm (arrows) persists despite loss of Notch in *N*^{55e11}/*Y* hemizygotes. (B) Expression of *rho-lacZ*, a reporter of Spi/Egfr activity. (C) pMAPK expression. (**D**) The *m8-GFP* reporter of Notch activation is activated in the pPI of *Egfr*^{f24} embryos. Scale bars: 20 μm.

Thus, there was no clear evidence of interdependency between the Notch and Egfr pathways or for cross-talk being essential for correct IPC NB specification.

We also examined mutants for Phyllopod (Phyl) and Charlatan (Chn), two factors essential for cell fate specification in the *Drosophila* eye and peripheral nervous system, where they mediate cross-talk between Notch and Egfr (Dickson et al., 1995; Pi et al., 2004; Escudero et al., 2005; Tsuda et al., 2006; Nagaraj and Banerjee, 2009). Phyl is essential for Notch-mediated induction of photoreceptor R7 fate, where it targets the transcriptional repressor Tramtrack (Ttk) for degradation. Loss of any of these three factors did not disrupt specification of the IPC NB lineage or pPIm cell survival (see Fig. S6A-D in the supplementary material). Together, the results indicated that Egfr and Notch need not cross-talk through Phyl, Ttk or Chn to specify the IPC NB identity.

Regional specification of a prepattern for the IPC NB equivalence group

Our results support a model in which the pPIm cells are the only cells of the Pdm NE that harbor the developmental potential to produce IPC lineages. We hypothesized that the IPC NB lineage identity could be conferred by the combinatorial activity of transcription factors and growth factor signals with regulatory activities that intersect within the pPIm to define a unique regulatory state, or 'prepattern', for the placode equivalence group.

By virtue of their intersecting expression in the pPIm, Chx1 and Cas were obvious candidates for prepattern factors. We examined *Chx1*^{A23} homozygous null mutant embryos that express an N-terminal fragment of the Chx1 protein localized to the cytoplasm, which permitted us to follow the fate of the Chx1^{+} cells (Erclik et al., 2008). We observed that the pPIm was specified, whereas the IPC NB was not (10/10 cases; see Fig. S7B and compare with control in S7A in the supplementary material). The IPCs were also absent from the PI of *Chx1*^{A23} first instar larval brains (see Fig. S7D and compare with control in S7C in the supplementary material). Furthermore, no Dimm^{+} NSCs formed at the position of the bilateral 10-12 Dac^{+} IPC NB lineages in *Chx1*^{A23} mutants (5/5 cases; see Fig. S7D and compare with control in S7C in the supplementary material). Together, these results indicate that Chx1 is essential for specification of the IPC NB identity and for development of any Dimm^{+} NSCs from the pPIm. Curiously, the Dac^{+} NSC lineage from the adjacent PI placode, which was positioned at the anterior tip of the Chx1^{+} domain, was specified in *Chx1*^{A23} mutants (see Fig. S7B, arrowheads, in the supplementary material), suggesting that the role of Chx1 as a prepattern determinant might be essential only for the pPIm placode.

By contrast, *cas*^{24} homozygous null mutant embryos (Cui and Doe, 1992) specified the IPC NB normally (7/7 cases; see Fig. S7E in the supplementary material). Thus, although Cas is a definitive marker of the pPIm, it is not an essential regulator of IPC NB identity.

In addition to intrinsic prepattern factors, we examined growth factor signals previously implicated in the patterning of the PI and head midline epidermis. TGFβ signaling via Decapentaplegic (Dpp) and Hedgehog (Hh) both act at the dorsal midline to specify the dorsal midline epidermis (Chang et al., 2001). Interestingly, we found that neither Dpp nor Hh signaling was essential for regional specification of the pPIm prepattern or for specification of the IPC NB lineage (see Fig. S7F,G in the supplementary material).

DISCUSSION

Key steps of placode development

Our observations provide a framework for understanding several key features of placodal neurogenesis in the Pdm; the steps in placode development are summarized as follows and are diagrammed in Fig. 6. The NE placode, comprising roughly eight cells, with its underlying gene regulatory network, appears to be highly specialized to serial specify a range of distinct neural stem cell identities, beginning from an initial state of equivalent

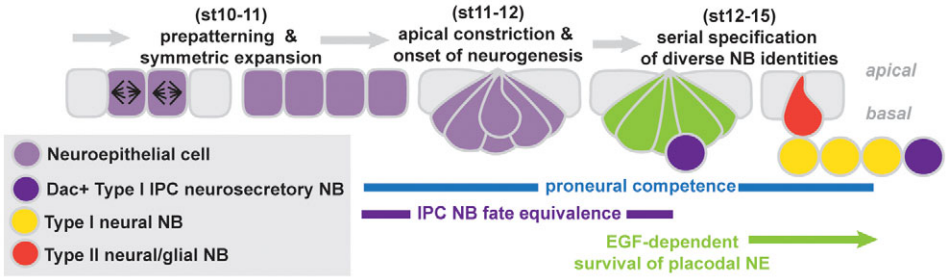

Fig. 6. Model for serial specification of NB identities from the *Drosophila* pPIm. Temporal progression of major developmental events in the pPIm is displayed from left to right, with corresponding stages indicated (see Discussion for details). The various cell types are color coded. The blue bar designates the extended period of proneural competence seen in the Pdm NE. The purple bar designates the period during which pPIm cells are competent to adopt the IPC NB fate. The green arrow designates the period following IPC NB specification during which the pPIm NE is dependent on Egfr activity for survival.

developmental potential. In the case of the pPIm, the initial state of competence is to form IPC NBs. The first indication that the pPIm had acquired prepattern identity was the synchronized round of cell division we observed before placode morphogenesis at the 4-cell pPIm stage. After the expansion to the 8-cell stage, the cells entered a cell cycle arrest and formed a neurogenic placode; the pPIm then initiated a lengthy proneural competence period as the various NB identities were produced. Our mutant and temperature shift analysis of Notch signaling suggested that a window of competence for the IPC NB fate exists from the time the pPIm expanded to eight cells and acquired proneural competence until the time that IPC NB fate was normally specified (the time that it became Dac$^+$). At roughly this point, the pPIm became dependent on Spi/Egfr activity to promote the survival of NE cells not yet specified as NBs. This Egfr-dependent specification period then extended through stage 15, while alternative NB identities were specified. Neurogenesis then ended with the specification of the single Type II NB fate. A summary of all phenotypes is shown in Fig. S8 in the supplementary material.

Parallels with photoreceptor R8 specification

Among the well-studied examples of *Drosophila* neurogenesis, perhaps the most intriguing parallels are found between serial fate specification in the placodal pPIm and in the developing facets of the *Drosophila* retina, particularly between specification of the IPC NB and the R8 photoreceptor within each developing ommatidium. The R8 photoreceptor is the first of a series of photoreceptor and cone cell fates to be specified by progressive recruitment to an apically constricted cluster of twelve cells (Wolff and Ready, 1993). Each R8 cell, the ommatidium founder, is specified from a proneural R8 fate equivalence group generated by the activity of the bHLH factor Atonal (Ato) (Jarman et al., 1994), and is singled out by Notch-mediated lateral inhibition (Cagan and Ready, 1989). Although parallel with respect to specification from a proneural fate equivalence group, the pPIm NE requires activity of the AS-C for IPC NB specification whereas Ato is not essential (data not shown). In contrast to R8 specification from a proneural group, the photoreceptor R1-7 and the cone cell fates are locally recruited within an ommatidium through inductive and serial Notch and Egfr/receptor tyrosine kinase (RTK) signaling from R8 (Dickson and Hafen, 1993). Analogous to the pPIm and IPC NB specification, Egfr activity is not essential for proneural competence and specification of R8, but is essential for survival of all photoreceptor precursors, except for R8 (Dominguez et al., 1998). Egfr-mediated cell survival in the developing retina requires that the pathway activates MAPK by phosphorylation and that pMAPK in turn phosphorylates the proapoptotic factor Head involution defective (Hid; Wrinkled – FlyBase) (Bergmann et al., 1998). In normal Egfr signaling, phosphorylated Hid is targeted for degradation, which permits survival of the developing ommatidium (Bergmann et al., 1998; Kurada and White, 1998); cell survival is also promoted by the activity of Pnt1/2, which repress Hid expression (Kurada and White, 1998; Yang and Baker, 2003). It was previously reported that *hid* mRNA accumulates in a pan-placodal Pdm NE pattern in stage 12-13 embryos (Grether et al., 1995; Tomancak et al., 2002), yet we found that Pnt1/2 was not obviously essential for survival to stage 14 (see Fig. S5F in the supplementary material). This suggests that, in contrast to the retina, most of the anti-apoptotic activity of Egfr signaling is relatively independent of Pnt1/2; hence, it might act primarily through the action of pMAPK in the turnover of Hid. This hypothesis will need to be tested more fully in future studies.

Notch and Egfr function in the pPIm placode

Although there are many examples of systems in which Notch and Egfr activities are mutually antagonistic or cooperate in promoting cell fate decisions (for reviews, see Sundaram, 2005; Doroquez and Rebay, 2006), we found no evidence of a mutual dependence between Notch and Egfr activity states; either pathway became active in the absence of the other. Admittedly, from our experiments we could not definitively rule out all cross-talk between the two pathways. By contrast, other instances of neurogenesis in *Drosophila*, such as in the optic lobe (Yasugi et al., 2010) and notum macrochaete (Culi et al., 2001; Escudero et al., 2005), depend on Egfr activity to promote neurogenesis by activating *as-c* genes. In these contexts, the Egfr-dependent proneural state is antagonized by Notch activity. In the pPIm proneural region, it remains unclear from our experiments whether Egfr is essential for neurogenesis subsequent to the IPC NB, as the pPIm cells are lost with the loss of Egfr activity. Indeed, there is a potential parallel with neurogenesis of the abdominal chordotonal precursors, which do form in the absence of Egfr activity but then signal back to the epithelium via Spi to activate *ato* and extend neurogenesis, thereby recruiting additional chordotonal precursors (Lage et al., 1997; zur Lage and Jarman, 1999; zur Lage et al., 2004).

In conclusion, the parallels between serial neural fate specification in the Pdm placode and in eye development raise the interesting possibility that some aspects of the two underlying gene

regulatory networks have points of overlap. If so, it is intriguing to consider whether distinct regions of proneural epithelia that express placode genes such as *sine oculis*, *Optix*, *Six4* and *eya*, were derived in evolution from a common ancestral neuroepithelial patterning circuit that was capable of serial specification. If this were the case, the implication would be that this mode of fate specification, in which diverse neuronal or neural stem cell identities are generated through local interactions in prepatterned cell groups, is more widely distributed than currently appreciated across animal phylogeny and vertebrate species. Hence, a deeper understanding of such a neural stem cell diversification mechanism will certainly aid efforts to control the differentiation of specific neural progenitor fates in vitro.

Acknowledgements
We thank Dr B. Grillo-Hill and A. Marusich for their contribution to the analysis of the *Chx1*^{A23} mutant; J. Wu for generating the Six4 antibody; Drs S. Bray, R. Hewes, P. Taghert, Y. N. Jan, J. Skeath, H. Lipshitz, T. Erclik, J. Posakony, J. Modollel, S. Campuzano, M. Rand, E. Bier, the Bloomington Stock Center and Developmental Studies Hybridoma Bank for stocks and reagents; and Drs A. Kriegstein, V. Hartenstein, R. Derynck, K. Brückner, T. Nystul, L. Kockel and J. Kumar for helpful comments and discussion. A special thanks to S. Celniker for many helpful discussions and for sharing unpublished data and reagents. This work was supported with funds from NIH RO1-DK069492, the UCSF Diabetes Center and the Eli and Edythe Broad Center of Regeneration Medicine and Stem Cell Research at UCSF.

Competing interests statement
The authors declare no competing financial interests.

Supplementary material
Supplementary material for this article is available at
http://dev.biologists.org/lookup/suppl/doi:10.1242/dev.055681/-/DC1

References

Bello, B. C., Izergina, N., Caussinus, E. and Reichert, H. (2008). Amplification of neural stem cell proliferation by intermediate progenitor cells in Drosophila brain development. *Neural Dev.* **3**, 5.
Bergmann, A., Agapite, J., McCall, K. and Steller, H. (1998). The Drosophila gene hid is a direct molecular target of Ras-dependent survival signaling. *Cell* **95**, 331-341.
Bhat, K. M. (1999). Segment polarity genes in neuroblast formation and identity specification during Drosophila neurogenesis. *BioEssays* **21**, 472-485.
Bier, E., Jan, L. Y. and Jan, Y. N. (1990). rhomboid, a gene required for dorsoventral axis establishment and peripheral nervous system development in Drosophila melanogaster. *Genes Dev.* **4**, 190-203.
Bier, E., Vaessin, H., Younger-Shepherd, S., Jan, L. Y. and Jan, Y. N. (1992). deadpan, an essential pan-neural gene in Drosophila, encodes a helix-loop-helix protein similar to the hairy gene product. *Genes Dev.* **6**, 2137-2151.
Boone, J. Q. and Doe, C. Q. (2008). Identification of Drosophila type II neuroblast lineages containing transit amplifying ganglion mother cells. *Dev. Neurobiol.* **68**, 1185-1195.
Bowman, S. K., Rolland, V., Betschinger, J., Kinsey, K. A., Emery, G. and Knoblich, J. A. (2008). The tumor suppressors Brat and Numb regulate transit-amplifying neuroblast lineages in Drosophila. *Dev. Cell* **14**, 535-546.
Broadus, J., Skeath, J. B., Spana, E. P., Bossing, T., Technau, G. and Doe, C. Q. (1995). New neuroblast markers and the origin of the aCC/pCC neurons in the Drosophila central nervous system. *Mech. Dev.* **53**, 393-402.
Cagan, R. L. and Ready, D. F. (1989). Notch is required for successive cell decisions in the developing Drosophila retina. *Genes Dev.* **3**, 1099-1112.
Campos-Ortega, J. A. and Hartenstein, V. (1985). *The Embryonic Development of Drosophila melanogaster*. Berlin: Springer-Verlag.
Castro, B., Barolo, S., Bailey, A. M. and Posakony, J. W. (2005). Lateral inhibition in proneural clusters: cis-regulatory logic and default repression by Suppressor of Hairless. *Development* **132**, 3333-3344.
Chang, T., Mazotta, J., Dumstrei, K., Dumitrescu, A. and Hartenstein, V. (2001). Dpp and Hh signaling in the Drosophila embryonic eye field. *Development* **128**, 4691-4704.
Clifford, R. J. and Schupbach, T. (1989). Coordinately and differentially mutable activities of torpedo, the Drosophila melanogaster homolog of the vertebrate EGF receptor gene. *Genetics* **123**, 771-787.
Cui, X. and Doe, C. Q. (1992). ming is expressed in neuroblast sublineages and regulates gene expression in the Drosophila central nervous system. *Development* **116**, 943-952.
Culi, J., Martin-Blanco, E. and Modolell, J. (2001). The EGF receptor and N signalling pathways act antagonistically in Drosophila mesothorax bristle patterning. *Development* **128**, 299-308.
de Velasco, B., Mandal, L., Mkrtchyan, M. and Hartenstein, V. (2006). Subdivision and developmental fate of the head mesoderm in Drosophila melanogaster. *Dev. Genes Evol.* **216**, 39-51.
de Velasco, B., Erclik, T., Shy, D., Sclafani, J., Lipshitz, H., McInnes, R. and Hartenstein, V. (2007). Specification and development of the pars intercerebralis and pars lateralis, neuroendocrine command centers in the Drosophila brain. *Dev. Biol.* **302**, 309-323.
Dickson, B. and Hafen, E. (1993). Genetic dissection of eye development in Drosophila. In *The Development of Drosophila melanogaster*, Vol. 2. (ed. M. Bate and A. Martinez Arias), pp. 1327-1362. Plainview, NY: Cold Spring Harbor Laboratory Press.
Dickson, B. J., Dominguez, M., van der Straten, A. and Hafen, E. (1995). Control of Drosophila photoreceptor cell fates by phyllopod, a novel nuclear protein acting downstream of the Raf kinase. *Cell* **80**, 453-462.
Dominguez, M., Wasserman, J. D. and Freeman, M. (1998). Multiple functions of the EGF receptor in Drosophila eye development. *Curr. Biol.* **8**, 1039-1048.
Doroquez, D. B. and Rebay, I. (2006). Signal integration during development: mechanisms of EGFR and Notch pathway function and cross-talk. *Crit. Rev. Biochem. Mol. Biol.* **41**, 339-385.
Dumstrei, K., Nassif, C., Abboud, G., Aryai, A. and Hartenstein, V. (1998). EGFR signaling is required for the differentiation and maintenance of neural progenitors along the dorsal midline of the Drosophila embryonic head. *Development* **125**, 3417-3426.
Erclik, T., Hartenstein, V., Lipshitz, H. D. and McInnes, R. R. (2008). Conserved role of the Vsx genes supports a monophyletic origin for bilaterian visual systems. *Curr. Biol.* **18**, 1278-1287.
Escudero, L. M., Caminero, E., Schulze, K. L., Bellen, H. J. and Modolell, J. (2005). Charlatan, a Zn-finger transcription factor, establishes a novel level of regulation of the proneural achaete/scute genes of Drosophila. *Development* **132**, 1211-1222.
Grether, M. E., Abrams, J. M., Agapite, J., White, K. and Steller, H. (1995). The head involution defective gene of Drosophila melanogaster functions in programmed cell death. *Genes Dev.* **9**, 1694-1708.
Heitzler, P. and Simpson, P. (1991). The choice of cell fate in the epidermis of Drosophila. *Cell* **64**, 1083-1092.
Hewes, R. S., Park, D., Gauthier, S. A., Schaefer, A. M. and Taghert, P. H. (2003). The bHLH protein Dimmed controls neuroendocrine cell differentiation in Drosophila. *Development* **130**, 1771-1781.
Izergina, N., Balmer, J., Bello, B. and Reichert, H. (2009). Postembryonic development of transit amplifying neuroblast lineages in the Drosophila brain. *Neural Dev.* **4**, 44.
Jarman, A. P., Grell, E. H., Ackerman, L., Jan, L. Y. and Jan, Y. N. (1994). Atonal is the proneural gene for Drosophila photoreceptors. *Nature* **369**, 398-400.
Kawamura, K., Kouki, T., Kawahara, G. and Kikuyama, S. (2002). Hypophyseal development in vertebrates from amphibians to mammals. *Gen. Comp. Endocrinol.* **126**, 130-135.
Klaes, A., Menne, T., Stollewerk, A., Scholz, H. and Klambt, C. (1994). The Ets transcription factors encoded by the Drosophila gene pointed direct glial cell differentiation in the embryonic CNS. *Cell* **78**, 149-160.
Kumar, J. P., Tio, M., Hsiung, F., Akopyan, S., Gabay, L., Seger, R., Shilo, B. Z. and Moses, K. (1998). Dissecting the roles of the Drosophila EGF receptor in eye development and MAP kinase activation. *Development* **125**, 3875-3885.
Kurada, P. and White, K. (1998). Ras promotes cell survival in Drosophila by downregulating hid expression. *Cell* **95**, 319-329.
Lage, P., Jan, Y. N. and Jarman, A. P. (1997). Requirement for EGF receptor signalling in neural recruitment during formation of Drosophila chordotonal sense organ clusters. *Curr. Biol.* **7**, 166-175.
Larkin, M. K., Holder, K., Yost, C., Giniger, E. and Ruohola-Baker, H. (1996). Expression of constitutively active Notch arrests follicle cells at a precursor stage during Drosophila oogenesis and disrupts the anterior-posterior axis of the oocyte. *Development* **122**, 3639-3650.
Lehmann, R., Jimenez, F., Dietrich, U. and Camposortega, J. A. (1983). On the phenotype and development of mutants of early neurogenesis in Drosophila-melanogaster. *Roux's Arch. Dev. Biol.* **192**, 62-74.
Lichtneckert, R. and Reichert, H. (2008). Anteroposterior regionalization of the brain: genetic and comparative aspects. *Adv. Exp. Med. Biol.* **628**, 32-41.
Markakis, E. A. (2002). Development of the neuroendocrine hypothalamus. *Front. Neuroendocrinol.* **23**, 257-291.
Martin-Bermudo, M. D., Martinez, C., Rodriguez, A. and Jimenez, F. (1991). Distribution and function of the lethal of scute gene product during early neurogenesis in Drosophila. *Development* **113**, 445-454.
Nagaraj, R. and Banerjee, U. (2009). Regulation of Notch and Wingless signalling by phyllopod, a transcriptional target of the EGFR pathway. *EMBO J.* **28**, 337-346.
Park, D., Veenstra, J. A., Park, J. H. and Taghert, P. H. (2008). Mapping peptidergic cells in Drosophila: where DIMM fits in. *PLoS ONE* **3**, e1896.

Parks, A. L., Stout, J. R., Shepard, S. B., Klueg, K. M., Dos Santos, A. A., Parody, T. R., Vaskova, M. and Muskavitch, M. A. (2006). Structure-function analysis of delta trafficking, receptor binding and signaling in Drosophila. *Genetics* **174**, 1947-1961.
Pereanu, W. and Hartenstein, V. (2006). Neural lineages of the Drosophila brain: a three-dimensional digital atlas of the pattern of lineage location and projection at the late larval stage. *J. Neurosci.* **26**, 5534-5553.
Pi, H., Huang, S. K., Tang, C. Y., Sun, Y. H. and Chien, C. T. (2004). phyllopod is a target gene of proneural proteins in Drosophila external sensory organ development. *Proc. Natl. Acad. Sci. USA* **101**, 8378-8383.
Qian, X., Goderie, S. K., Shen, Q., Stern, J. H. and Temple, S. (1998). Intrinsic programs of patterned cell lineages in isolated vertebrate CNS ventricular zone cells. *Development* **125**, 3143-3152.
Rogge, R., Green, P. J., Urano, J., Horn-Saban, S., Mlodzik, M., Shilo, B. Z., Hartenstein, V. and Banerjee, U. (1995). The role of yan in mediating the choice between cell division and differentiation. *Development* **121**, 3947-3958.
Rulifson, E. J. and Blair, S. S. (1995). Notch regulates wingless expression and is not required for reception of the paracrine wingless signal during wing margin neurogenesis in Drosophila. *Development* **121**, 2813-2824.
Rulifson, E. J., Kim, S. K. and Nusse, R. (2002). Ablation of insulin-producing neurons in flies: growth and diabetic phenotypes. *Science* **296**, 1118-1120.
Schlosser, G. (2006). Induction and specification of cranial placodes. *Dev. Biol.* **294**, 303-351.
Schnepp, B., Grumbling, G., Donaldson, T. and Simcox, A. (1996). Vein is a novel component in the Drosophila epidermal growth factor receptor pathway with similarity to the neuregulins. *Genes Dev.* **10**, 2302-2313.
Scholz, H., Deatrick, J., Klaes, A. and Klämbt, C. (1993). Genetic dissection of *pointed*, a *Drosophila* gene encoding two ETS related proteins. *Genetics* **135**, 455-468.
Siegmund, T. and Korge, G. (2001). Innervation of the ring gland of Drosophila melanogaster. *J. Comp. Neurol.* **431**, 481-491.
Skeath, J. B. (1999). At the nexus between pattern formation and cell-type specification: the generation of individual neuroblast fates in the Drosophila embryonic central nervous system. *BioEssays* **21**, 922-931.
Skeath, J. B. and Carroll, S. B. (1992). Regulation of proneural gene expression and cell fate during neuroblast segregation in the Drosophila embryo. *Development* **114**, 939-946.
Skeath, J. B. and Thor, S. (2003). Genetic control of Drosophila nerve cord development. *Curr. Opin. Neurobiol.* **13**, 8-15.
Spencer, S. A., Powell, P. A., Miller, D. T. and Cagan, R. L. (1998). Regulation of EGF receptor signaling establishes pattern across the developing Drosophila retina. *Development* **125**, 4777-4790.
Sprecher, S. G., Reichert, H. and Hartenstein, V. (2007). Gene expression patterns in primary neuronal clusters of the Drosophila embryonic brain. *Gene Expr. Patterns* **7**, 584-595.
Struhl, G. and Basler, K. (1993). Organizing activity of wingless protein in Drosophila. *Cell* **72**, 527-540.
Sullivan, W., Ashburner, M. and Hawley, R. S. (2000). *Drosophila protocols*. Cold Spring Harbor, NY: Cold Spring Harbor Laboratory Press.
Sundaram, M. V. (2005). The love-hate relationship between Ras and Notch. *Genes Dev.* **19**, 1825-1839.
Technau, G. M. and Campos-Ortega, J. A. (1987). Cell autonomy of expression of neurogenic genes of Drosophila melanogaster. *Proc. Natl. Acad. Sci. USA* **84**, 4500-4504.
Technau, G. M., Berger, C. and Urbach, R. (2006). Generation of cell diversity and segmental pattern in the embryonic central nervous system of Drosophila. *Dev. Dyn.* **235**, 861-869.
Tomancak, P., Beaton, A., Weiszmann, R., Kwan, E., Shu, S., Lewis, S. E., Richards, S., Ashburner, M., Hartenstein, V., Celniker, S. E. et al. (2002). Systematic determination of patterns of gene expression during Drosophila embryogenesis. *Genome Biol.* **3**, RESEARCH0088.
Tsuda, L., Kaido, M., Lim, Y. M., Kato, K., Aigaki, T. and Hayashi, S. (2006). An NRSF/REST-like repressor downstream of Ebi/SMRTER/Su(H) regulates eye development in Drosophila. *EMBO J.* **25**, 3191-3202.
Urbach, R. and Technau, G. M. (2003). Segment polarity and DV patterning gene expression reveals segmental organization of the Drosophila brain. *Development* **130**, 3607-3620.
Urbach, R. and Technau, G. M. (2008). Dorsoventral patterning of the brain: a comparative approach. *Adv. Exp. Med. Biol.* **628**, 42-56.
Urbach, R., Schnabel, R. and Technau, G. M. (2003). The pattern of neuroblast formation, mitotic domains and proneural gene expression during early brain development in Drosophila. *Development* **130**, 3589-3606.
Urbach, R., Volland, D., Seibert, J. and Technau, G. M. (2006). Segment-specific requirements for dorsoventral patterning genes during early brain development in Drosophila. *Development* **133**, 4315-4330.
Urban, S., Lee, J. R. and Freeman, M. (2002). A family of Rhomboid intramembrane proteases activates all Drosophila membrane-tethered EGF ligands. *EMBO J.* **21**, 4277-4286.
Wang, S., Tulina, N., Carlin, D. L. and Rulifson, E. J. (2007). The origin of islet-like cells in Drosophila identifies parallels to the vertebrate endocrine axis. *Proc. Natl. Acad. Sci. USA* **104**, 19873-19878.
Whitlock, K. E. (2005). Origin and development of GnRH neurons. *Trends Endocrinol. Metab.* **16**, 145-151.
Wolff, T. and Ready, D. F. (1993). Pattern formation in the *Drosophila* retina. In *The Development of Drosophila melanogaster*, Vol. 2 (ed. M. Bate and A. Martinez Arias), pp. 1277-1325. Plainview, NY: Cold Spring Harbor Laboratory Press.
Yang, L. and Baker, N. E. (2003). Cell cycle withdrawal, progression, and cell survival regulation by EGFR and its effectors in the differentiating Drosophila eye. *Dev. Cell* **4**, 359-369.
Yasugi, T., Sugie, A., Umetsu, D. and Tabata, T. (2010). Coordinated sequential action of EGFR and Notch signaling pathways regulates proneural wave progression in the Drosophila optic lobe. *Development* **137**, 3193-3203.
Younossi-Hartenstein, A., Nassif, C., Green, P. and Hartenstein, V. (1996). Early neurogenesis of the Drosophila brain. *J. Comp. Neurol.* **370**, 313-329.
Younossi-Hartenstein, A., Green, P., Liaw, G. J., Rudolph, K., Lengyel, J. and Hartenstein, V. (1997). Control of early neurogenesis of the Drosophila brain by the head gap genes tll, otd, ems, and btd. *Dev. Biol.* **182**, 270-283.
zur Lage, P. and Jarman, A. P. (1999). Antagonism of EGFR and notch signalling in the reiterative recruitment of Drosophila adult chordotonal sense organ precursors. *Development* **126**, 3149-3157.
zur Lage, P. I., Powell, L. M., Prentice, D. R., McLaughlin, P. and Jarman, A. P. (2004). EGF receptor signaling triggers recruitment of Drosophila sense organ precursors by stimulating proneural gene autoregulation. *Dev. Cell* **7**, 687-696.